Spectral dependence of the ultrafast optical response of nonspherical gold nanoparticles

Yannick Guillet, Eric Charron, and Bruno Palpant*
Institut des Nano-Sciences de Paris, Centre National de la Recherche Scientifique, Université Pierre et Marie Curie–Paris 6, UMR 7588, 140 rue de Lourmel, 75015 Paris, France
(Received 2 April 2009; published 22 May 2009)

The extension of the discrete dipole approximation (DDA) model to the calculation of the ultrafast transient optical response of metal nanoparticles, whatever their shape, is presented. For this, the DDA is combined with the resolution of the Boltzmann equation for the conduction electrons within the low-perturbation limit and the Rosei model for the metal band structure. This approach thus takes into account the athermal regime for the electron gas. It is then illustrated in the cases of gold nanospheres and nanopeanuts. The spectral dependence of the ultrafast response is shown to be very sensitive to the particle morphology, the surface plasmon resonance enhancing the transient modification of the interband transitions. These results are used to interpret spectrally resolved pump-probe measurements performed on a dense nanoparticle assembly, demonstrating selective-excitation and selective-detection processes.

DOI: 10.1103/PhysRevB.79.195432 PACS number(s): 78.67.Bf, 42.65.−k, 78.47.−p

Confinement of noble metals at a nanometric scale results in the appearance of the well-known surface plasmon resonance (SPR) in their optical spectrum, associated with the local enhancement of the oscillating electric field.[1] Understanding energy exchanges in noble metal nanoparticles under optical excitation is one of the main important points so as to control their optical properties. As these exchanges take place on a picosecond timescale,[2] femtosecond laser pump-probe experiments have turned out to be very suitable for getting insight into their dynamics.[3–5] The shape of metal nanoparticles as well as interactions between neighboring particles strongly influence the characteristics of their SPR (i.e., spectral position, width, and magnitude). For instance, for an electric field **E** polarized along the longest dimension of nonspherical particles such as nanorods[6] or gold dimers (i.e., two strongly interacting particles spatially very close),[7,8] the SPR usually located at 2.34 eV for a single gold sphere in silica is redshifted. For a gold dimer, this shift is maximum in the asymptotic case of a point contact between two spheres.[9,10] Besides, these morphological factors also influence the nano-object ultrafast transient optical response. Numerous experimental and theoretical works have shown that on a 100 ps timescale coherent vibration modes are strongly dependent on the shape of the nanoparticle[11–13] or on near-field effects due to interactions between neighboring particles.[14] In the same way, pump-probe experiments on gold nanorods[15,16] and gold nanoparticle aggregates[17] have highlighted that shape and/or interactions play a significant role in the spectral signature of the electron relaxation on a picosecond timescale. The spectral feature observed around the redshifted SPR has up to now been attributed to the only SPR transient broadening or frequency shift (due to the pulse-induced heating of the conduction electrons). However, the athermal regime[18] modifies the electron distribution far from the interband transition threshold and may also contribute to the ultrafast response far from this threshold. The calculation of the transient optical response for nano-objects of any shape or for interacting objects, taking into account the athermal regime, thus appears to be a relevant issue to be addressed. In this paper, we propose an original numerical approach allowing the determination of the ultrafast transient response of nonspherical nanoparticles in the low-perturbation regime. We then use computed time-dependent spectra to interpret results of pump-probe experiments carried out on a dense nanocomposite assembly. Invoking the transient modification of interband transitions enables us to demonstrate the high sensitivity of the spectral dependence of the transient optical response to the detailed morphology of the excited nano-objects. We finally discuss the possible additional contribution of the modification of the dielectric function intraband component to the ultrafast response.

The discrete dipole approximation (DDA) has been used to preliminarily determine the stationary optical response of gold nanoparticles having two different morphologies: an isolated spherical particle and two slightly overlapped ones forming a peanut. DDA combines no specific restriction on the shape of the nanoparticles and quite low-computation times.[19] The numerical code DDSCAT developed by Draine and Flatau[20] has been processed. The resulting spectra of the optical absorption cross-section (σ) of a 10-nm-diameter sphere (gray line) and two 10-nm-diameter spheres overlapping over 3 nm (solid and dashed black lines for a field polarization along and orthogonal to the interparticle axis, respectively) are reported on Fig. 1. Gray and dashed black spectra are roughly similar; in the following both configurations will be assumed to have the same optical response. The spectrum related to the peanut with **E** polarized along its

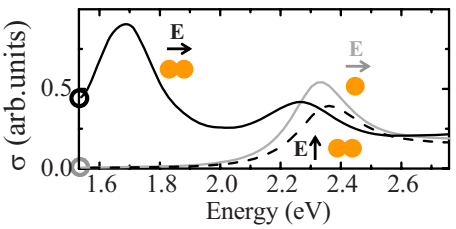

FIG. 1. (Color online) Computed spectrum of the absorption cross-section σ for a single gold nanosphere (gray curve) and a gold nanopeanut (solid and dashed black curves for an electric field **E** polarized parallel and orthogonally to the peanut long axis, respectively) as calculated by the DDA.

long axis presents two SPRs at 1.70 and 2.30 eV, the first one being associated with the oscillation of the free-electron gas over the whole peanut (like in a nanorod), and the other corresponding to its partial confinement in each initial sphere (like for hot spots in semicontinuous gold films).[9]

Let us now focus on the transient optical response of gold nanoparticles following the excitation by an ultrashort light pulse. This pump pulse (photon energy $\hbar\omega$=1.55 eV) is absorbed through intraband transitions and put the conduction-electron gas (described by a distribution function f) up to an out-of-equilibrium state. The dynamics of f has been computed by solving the Boltzmann equation. This has been done in the low-perturbation limit using a relaxation-time approximation[21] and taking into account the finite duration of the pump pulse[22] (for more details, see Ref. 23). It is assumed that the only interband part ε^{IB} of the dielectric function of gold, ε, is significantly perturbed.[24] The time evolution of ε^{IB} is calculated with the Rosei model.[23,25] The spectral and temporal behaviors $\varepsilon(\omega,\tau)$ of ε are obtained by adding the Drude susceptibility. To carry out DDA calculations, each nanoparticle is described by 25 000 dipoles. Spectral and time resolutions are 4 nm and 100 fs, respectively. Typical computation time is a few hours for each absorption cross-section spectrum (with a 10^{-5} error tolerance).

The dynamics of the optical response is calculated by considering a fixed incident-light intensity. The input energy in the source term of the Boltzmann equation is thus proportional to the absorption cross section, σ. The two points at the pump photon energy 1.55 eV in Fig. 1 highlight the value of σ for a sphere (σ_S) and a peanut with **E** parallel to its long axis (σ_P): σ_P=70σ_S. Depending on the morphology considered, we then obtain two dynamical behaviors of ε: the one for a sphere, $\varepsilon_S(\omega,\tau)$, and the other for a peanut, $\varepsilon_P(\omega,\tau)$. The former corresponds to an excitation magnitude 70 times lower than for the latter in the calculation of f. The spectrum of σ is then computed by using the DDA in both morphologies and for each delay τ.

We calculate the differential absorption cross-section $\Delta\sigma/\sigma(\omega,\tau)$, i.e., the relative variation of σ induced by the pump pulse, for a single sphere [Figs. 2(a)–2(c)] and a peanut [Figs. 3(a)–3(c)]. The linear absorption spectra of Fig. 1 have been reported for sake of discussion in Figs. 2(a) and 3(a). Figures 2(b) and 3(b) display on a color scale the value of the transient absorption cross-section as a function of delay τ (vertical axis) and probe photon energy (horizontal axis). The transient absorption spectrum at its temporal maximum [dashed gray line in Figs. 2(b) and 3(b)] is reported on Figs. 2(c) and 3(c).

The spectral profile of the transient response for a single sphere obtained by this method is in very good agreement with experimental results reported in the literature for dilute media.[4,24] First, going from red to blue, $\Delta\sigma/\sigma$ is successively positive, negative, and positive again. Moreover, the magnitude of the positive peak at 2.50 eV is lower than the negative one at 2.35 eV [respectively, thin and thick arrows in Fig. 2(c)]. On the other hand, the transient response of the peanut turns out to be spectrally very different from the one of the sphere. Indeed, a negative $\Delta\sigma/\sigma$ appears between 1.65 and 2.00 eV. It is interesting to note that in our approach, and contrary to what is invoked in Refs. 15–17, this

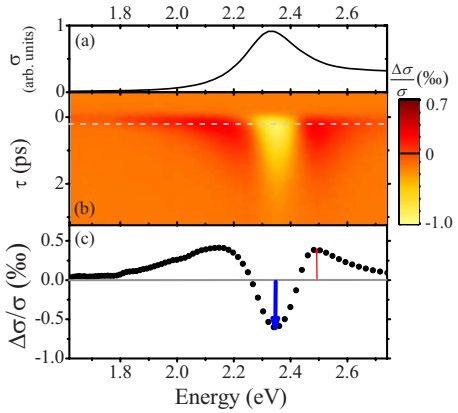

FIG. 2. (Color online) [(a)–(c)] Ultrafast optical response simulated by the coupled use of the Rosei model, the Boltzmann equation, and the DDA for a single gold nanosphere. (a) Stationary absorption cross-section reported from Fig. 1. (b) Transient differential absorption cross-section; vertical axis: pump-probe delay τ; horizontal axis: probe photon energy; and color scale: magnitude of the transient absorption. (c) Temporal maximum [along the dashed gray line on (b)] of the transient absorption over the whole probe spectral range.

spectral signature originates only from the transient modification of the interband transition spectrum, magnified by the field enhancement associated with the nanopeanut SPR located at 1.70 eV. Furthermore, the relative weight of the positive and negative peak magnitudes [respectively, thin and thick arrows in Fig. 3(c)] is inverted as compared with the one of the sphere. Finally, vertical scales of Figs. 2(c) and 3(c) reveal that the amplitude of these peaks is greater for a peanut than for a sphere by more than 1 order of magnitude.

In order to illustrate these differences, time-resolved experiments have been performed on a dense gold nanoparticle assembly consisting of a broad and continuous distribution of local morphologies, ranging from well separated particles to close-packed ones (like, for example, dimers) or nonspherical particles such as nanopeanuts, resulting from the

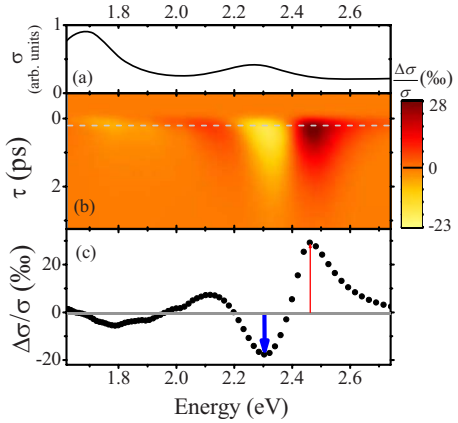

FIG. 3. (Color online) [(a)–(c)] Ultrafast optical response simulated by the coupled use of the Rosei model, the Boltzmann equation, and the DDA for a gold nanopeanut. **E** is polarized along the long symmetry axis. Organization of graphics is the same as the one of Fig. 2.

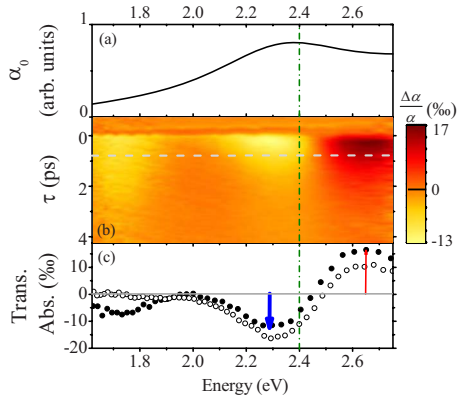

FIG. 4. (Color online) (a) Experimental spectrum of the linear absorption coefficient α_0 of the $Au:SiO_2$ thin film with $p=22\%$. Organization of graphics in (b) and (c) for the experimental differential absorption is the same as the one of Fig. 2. (c) Solid (open) circles correspond to experimental results with a pump photon energy at 1.55 eV (3.10 eV). The vertical dash-dotted line denotes the interband transition threshold of gold, $\hbar\omega_{IB}$.

coalescence of two initial spheres. This $Au:SiO_2$ nanocomposite thin film with $p=22\%$ gold volume fraction has been elaborated by radio frequency sputtering.[26] Gold particles of about 3 nm diameter are randomly spread in the host medium. The optical-absorption coefficient spectrum is displayed in Fig. 4(a). The SPR band is located at ~2.40 eV. It presents a quite large width mainly due to the inhomogeneous broadening which results from the addition of a continuous ensemble of spectra roughly ranging from the solid line to the dashed one of Fig. 1(a). Let us mention that finite-size effects, which are not included in our calculation, contribute also to the width of the SPR band in experimental spectra.[27]

Time-resolved experiments were carried out with a spectroscopic pump-probe setup. The light source is an amplified laser (Spectra Physics) delivering 120 fs pulses at 1.55 eV. The pulsed beam is split into two parts: a monochromatic and intense one excites the sample (pump pulse) while the other (only 5% of the incident power) is focused onto a sapphire plate to generate a highly stable white-light continuum (extending from 1.65 to 2.75 eV). This is used as a probe beam to measure the transient absorption spectra, i.e., the relative variation of the sample absorption induced by the pump pulse. A high-precision mechanical-translation stage (Aerotech) is used to control at the femtosecond scale the delay between probe and pump pulses, τ. The detection stage consists of a charge coupled device camera (Andor) coupled to a spectrometer (Horiba Jobin-Yvon). The use of a reference beam allows detecting transient absorption as low as 0.1%. The main advantage of this setup is to get, with only one acquisition, the ultrafast response of the sample over a wide spectral range.

The spectrally resolved pump-probe signal measured on the sample following the excitation by a ~1 GW cm^{-2} peak-intensity pump pulse at 1.55 eV is displayed on Fig. 4, where the graphics are organized as those in Figs. 2 and 3. Ultrafast transient response of such highly concentrated media has rarely been dealt with in the literature.[17] The transient absorption spectral profile in the vicinity of the interband transition threshold $\hbar\omega_{IB}$ (vertical dash-dotted green line) is consistent with previous experimental results reported by others on diluted media, typically with p lower than 1%.[4,24] However, two additional features are present in our case. First, a negative transient absorption appears between ~1.6 and 1.9 eV. Second, the magnitude of the positive peak at 2.65 eV is larger than the negative one at 2.30 eV [see arrows on Fig. 4(c)].

All these characteristics can be understood thanks to the preceding computation results (Figs. 2 and 3). Both *selective-excitation* and *selective-detection* processes have to be invoked:[16] (i) the SPR field enhancement in the different specific morphologies, like peanuts, reveals the modification of interband transitions in spectral domains where it is usually not amplified in the case of isolated spheres. This selective-detection process is responsible for the negative transient absorption observed between 1.70 and 1.90 eV (Fig. 4). This is in agreement with the results reported by Jain *et al.*[17] on the transient absorption of aggregates of gold nanoparticles. Such a spectral signature reveals the presence of a certain class of local morphologies in the medium. Although its influence is hidden in the stationary linear optical response, it is emphasized in the transient one by the selective-excitation process. (ii) The selective excitation is revealed by the magnitude of the experimental transient absorption around 1.70 eV. The presence in the material of a very small fraction of nanoparticles having an unusual specific morphology can nevertheless contribute significantly to the ultrafast optical response. Indeed, pump photons are absorbed preferentially by nanoparticles having a SPR energy close to $\hbar\omega$ [1.55 eV here, cf. black and gray points in Fig. 1]. The energy input per particle is then not homogeneous within the medium. To confirm this selective-excitation mechanism, we have carried out a pump-probe experiment with a pump beam at 3.10 eV photon energy. The negative transient absorption in the red part of the spectrum is then no longer present and the relative weight of the positive and negative peak magnitudes is inverted as compared to the 1.55 eV excitation [cf. open circles in Fig. 4(c)]. Let us note the absence in the experimental transient absorption of the positive peak at ~2.1 eV yet predicted by the simulations. This stems from the "ideal" situation chosen in our calculations, where only two extreme morphological cases (nanosphere and nanopeanut) are considered. As discussed above, the actual linear and nonlinear optical responses of our sample are the result of an ensemble average over a continuous distribution of local morphologies. Furthermore, quantum finite-size effects are not included in our simulations, which in fact would lead to the quenching and broadening of the SPR.[27]

Actually, the dielectric function ε is the sum of the interband component, ε^{IB}, and the intraband one, χ^D, usually described in noble metals by the Drude model. We have focused here on the perturbation of ε^{IB} following a subpicosecond optical excitation but the transient modification of χ^D could also contribute to the ultrafast optical response. This point could be especially relevant here since probe photons have an energy close to 1.5 eV, i.e., far below the interband threshold of gold ($\hbar\omega_{IB}\approx 2.4$ eV): in this spec-

tral range, ε is dominated by χ^D. The influence of the transient intraband component has been reported in the literature by several groups, with a specific interest for the ideal case of silver nanoparticles,[24,28] since their SPR lies in a spectral domain clearly separated from interband transitions ($\hbar\omega_{IB} \approx 4.0$ eV). The Vallée group carried out pump-probe measurements on silver nanospheres embedded in a silica matrix ($\hbar\omega_{SPR} \approx 2.9$ eV). They demonstrated that in the weak-perturbation regime the modification of the intraband component, which results in an enhancement of the electron-scattering processes, has to be included to fully describe the detailed spectral behavior of the transient transmission. However, their calculations also showed that, except from very close to the SPR frequency, the major contribution to the spectral signature stems by far from the modification of interband transitions [dashed line in Fig. 4b in Ref. 24] which corresponds to the one we have accounted for in our model. Moreover, Feldmann reported pump-probe experiments carried out on ellipsoidal silver nanoparticles in the strong-perturbation regime. The electron temperatures reached, and consequently the enhancement of electron-scattering processes, are expected to become important.[28] They concluded that the agreement between experimental results and theoretical predictions is much better if they only include the interband transition contribution rather than the only intraband one. These findings thus support the relevance of our approach in the present paper, the main aim of which was to underline through novel model and experiments the complex interplay between the electron relaxation in metal nanoparticles and the spectral signature of the medium transient response.

In summary, we have presented an original numerical method allowing to determine the ultrafast transient optical response of noble metal nanoparticles of any shape with affordable computation time. This method, which takes into account the athermal regime, associates the numerical resolution of the Boltzmann equation for the conduction electrons, the Rosei model for the dielectric function, and the DDA. This has been illustrated in the case of gold nanosphere and nanopeanut. The spectral characteristics of the transient absorption have been shown to be strongly dependent on the nano-object morphology due to a complex interplay between the modification of the interband transition probability and the way this modification is enhanced by the SPR. The theoretical transient spectra have finally been used to interpret the results of spectrally resolved pump-probe experiments performed on a highly concentrated medium through both selective-excitation and selective-detection processes. Without the necessity of invoking any transient broadening or shift of the SPR experimental results were correctly predicted by our model. It would be interesting to refine it by including the enhancement of electron-scattering processes through the modification of intraband transitions. We have thus demonstrated the sensitivity of time-resolved spectral measurement results to the detailed local morphology of the probed medium, whereas in conventional linear optical measurements such information can be hidden.

The French *Agence Nationale de la Recherche* (program ANR/PNANO 2006, project EThNA) is acknowledged for its financial support.

*bruno.palpant@upmc.fr

[1] C. F. Bohren and D. R. Huffman, *Absorption and Scattering of Light by Small Particles* (Wiley, Interscience, New York, 1983).
[2] C. K. Sun, F. Vallée, L. Acioli, E. P. Ippen, and J. G. Fujimoto, Phys. Rev. B **48**, 12365 (1993).
[3] J.-Y. Bigot, J.-C. Merle, O. Cregut, and A. Daunois, Phys. Rev. Lett. **75**, 4702 (1995).
[4] M. Perner, P. Bost, U. Lemmer, G. von Plessen, J. Feldmann, U. Becker, M. Mennig, M. Schmitt, and H. Schmidt, Phys. Rev. Lett. **78**, 2192 (1997).
[5] C. Voisin, D. Christofilos, N. Del Fatti, F. Vallée, B. Prével, E. Cottancin, J. Lermé, M. Pellarin, and M. Broyer, Phys. Rev. Lett. **85**, 2200 (2000).
[6] C. Noguez, J. Phys. Chem. C **111**, 3806 (2007).
[7] W. Gotschy, K. Vonmetz, A. Leitner, and F. R. Aussenegg, Opt. Lett. **21**, 1099 (1996).
[8] B. Palpant, Y. Guillet, M. Rashidi-Huyeh, and D. Prot, Gold Bull. **41**, 105 (2008).
[9] I. Romero, J. Aizpurua, G. W. Bryant, and F. J. García de Abajo, Opt. Express **14**, 9988 (2006).
[10] J. Lermé, C. Bonnet, M. Broyer, E. Cottancin, S. Marhaba, and M. Pellarin, Phys. Rev. B **77**, 245406 (2008).
[11] H. Petrova, C.-H. Lin, S. de Liejer, M. Hu, J. M. McLellan, A. R. Siekkinen, B. J. Wiley, M. Marquez, Y. Xia, J. E. Sader, and G. V. Hartland, J. Chem. Phys. **126**, 094709 (2007).
[12] M. Perner, S. Gresillon, J. März, G. von Plessen, J. Feldmann, J. Porstendorfer, K.-J. Berg, and G. Berg, Phys. Rev. Lett. **85**, 792 (2000).
[13] C. Guillon, P. Langot, N. Del Fatti, F. Vallée, A. S. Kirakosyan, T. V. Shahbazyan, T. Cardinal, and M. Treguer, Nano Lett. **7**, 138 (2007).
[14] W. Huang, W. Qian, P. K. Jain, and M. A. El-Sayed, Nano Lett. **7**, 3227 (2007).
[15] S. Link, C. Burda, M. B. Mohamed, B. Nikoobakht, and M. A. El-Sayed, Phys. Rev. B **61**, 6086 (2000).
[16] S. Park, M. Pelton, M. Liu, P. Guyot-Sionnest, and N. F. Scherer, J. Phys. Chem. C **111**, 116 (2007).
[17] P. K. Jain, W. Qian, and M. A. El-Sayed, J. Phys. Chem. B **110**, 136 (2006).
[18] W. S. Fann, R. Storz, H. W. K. Tom, and J. Bokor, Phys. Rev. Lett. **68**, 2834 (1992).
[19] B. T. Draine and P. J. Flatau, J. Opt. Soc. Am. A Opt. Image Sci. Vis **11**, 1491 (1994).
[20] B. T. Draine and P. J. Flatau, User Guide to the Discrete Dipole Approximation Code DDSCAT 7.0, http://arxiv.org/abs/0809.0337v5 (2008).
[21] V. E. Gusev and O. B. Wright, Phys. Rev. B **57**, 2878 (1998).
[22] N. Del Fatti, C. Voisin, M. Achermann, S. Tzortzakis, D. Christofilos, and F. Vallée, Phys. Rev. B **61**, 16956 (2000).
[23] Y. Guillet, M. Rashidi-Huyeh, and B. Palpant, Phys. Rev. B **79**,

045410 (2009).
[24] N. Del Fatti and F. Vallée, Appl. Phys. B: Lasers Opt. **73**, 383 (2001).
[25] M. Guerrisi, R. Rosei, and P. Winsemius, Phys. Rev. B **12**, 557 (1975).
[26] N. Pinçon-Roetzinger, D. Prot, B. Palpant, E. Charron, and S. Debrus, Mater. Sci. Eng., C **19**, 51 (2002).
[27] B. Palpant, B. Prével, J. Lermé, E. Cottancin, M. Pellarin, M. Treilleux, A. Perez, J.-L. Vialle, and M. Broyer, Phys. Rev. B **57**, 1963 (1998).
[28] G. von Plessen, M. Perner, and J. Feldmann, Appl. Phys. B: Lasers Opt. **71**, 381 (2000).